Digital Backpropagation for Optical Path Monitoring: Loss Profile and Passband Narrowing Estimation

Takeo Sasai [1], Masanori Nakamura[1], Etsushi Yamazaki, Shuto Yamamoto, Hideki Nishizawa, and Yoshiaki Kisaka

[1] NTT Network Innovation Laboratories, takeo.sasai.cp@hco.ntt.co.jp

Abstract *We propose an optical-path backpropagation algorithm that enables monitoring the loss profile along fibres and the individual frequency-detuning of cascaded optical filters in multi-span links. The method is based on the learning of backpropagation with complex-valued FIR filters and successfully identifies an anomaly optical filter.*

Introduction

Scaling transmitted data capacity in optical fibre transmission is becoming more and more challenging. Spectral efficiency (SE) enhancement by seeking higher order QAM imposes a severe requirement for signal-to-noise ratio (SNR) and the capacity expansion rate is limited to logarithmic increase with SNR[1]. As another approach to enhance SE, arranging wavelength-division multiplexed (WDM) channels tightly and reducing unused and wasted bandwidth are also essential[2].

In such a less guard-band system, signals are vulnerable to passband narrowing (PBN) due to the misalignment or the bandwidth deviation of optical filters (e.g. wavelength selective switch, WSS) in ROADM systems[3]. Recent WSS can tune its bandwidth and its central frequency as fine as a few GHz[4] and we can minimize the PBN penalty if these parameters are tailored to its incoming signals. However, it is challenging to identify the frequency-detuned filter among multiple number of cascaded filters and estimate its frequency shift and shape because concatenated linear systems (the overall responses of two optical filters) are not separable.

In this paper, we demonstrate the identification of frequency-detuned filters and estimation of its deviated frequency by utilizing the fibre nonlinearity (self-phase modulation) between optical filters to separately estimate filter responses. The loss profile along the multi-span link is also obtained simultaneously. Our tested link has three spans with two nodes, in which the centre frequencies of optical filters are varied to emulate the PBN. The intentionally deviated filter is detected and its shifted frequency is estimated only by receiver-side signal processing. The method is based on the learning of the optical-path backpropagation, which is a closer model to actual transmission systems than traditional digital backpropagation[5] (DBP).

Principle

The responses of two optical filters are basically cannot be separated at the receiver side when the system is a completely linear system. However, we can distinguish their responses by leveraging fibre nonlinearity between filters since linear and nonlinear phenomena are non-commutative.

The method is an extended version of our previous work[6] that enabled monitoring the loss and dispersion profile along the multi-span fibres by learning the DBP[7]. In this time, we insert the

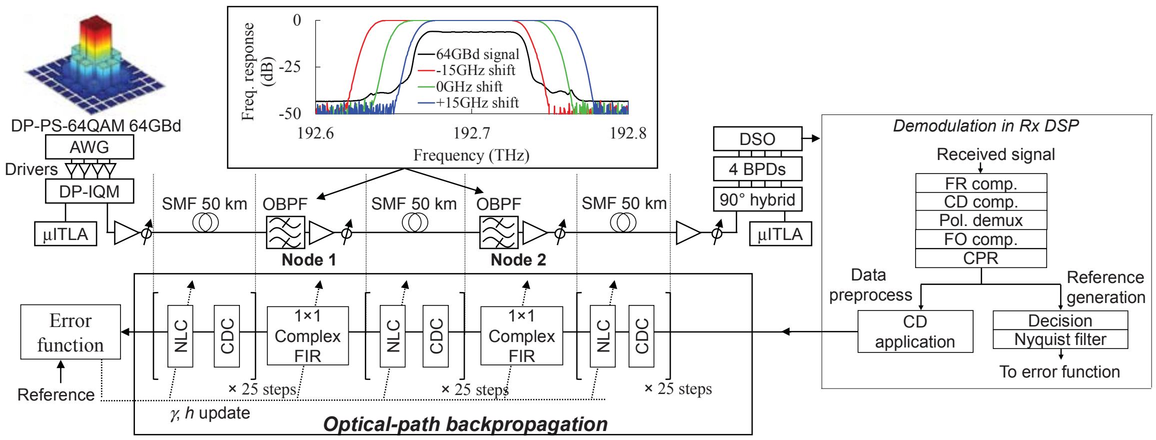

Fig. 1. Experimental setup and block diagram of Rx DSP and backpropagation with complex FIR filters that emulate OBPFs in nodes.

complex-valued finite impulse response (FIR) filter into our DBP. The block diagram of the proposed method is shown at the bottom of Fig. 1. First, input signals propagates through the standard DBP for one span with arbitrary initial values of γ_k, where k = 1, 2,…N is the k-th step of DBP. The DBP consists of the iteration of nonlinear compensation (NLC) and chromatic dispersion compensation (CDC). Before being input to the second span, the signals are filtered by a 1×1 complex FIR filter h, which corresponds to the inverse transfer function of the optical filter in a node. The initial values of the taps are set to the real-valued impulse function. The filter needs to be complex values to emulate the asymmetric response of the deviated optical filter. We define h_1 and h_2 as the FIR filters that compensates for the PBN of the first and second optical filter, respectively. Then, the same process continues until the signals digitally reach the transmitter-side (Tx) end.

The mean square error (MSE) $E = \Sigma|y(t) - d(t)|^2$ is calculated as an error function, where $y(t)$ denotes the back-propagated signal and $d(t)$ the reference signal. The reference signal is generated by the normal demodulation process in the Rx digital signal processing (DSP). This is a least square problem and the task is to find the optimum value of γ_k and h that minimize the MSE, which can be solved by the gradient descent. For the update of the coefficients γ_k and h, Adam algorithm[8] is used. The partial differentiations $\partial E/\partial \gamma_k$ and $\partial E/\partial h$ are calculated from differentiations of the output with respect to the input in each block (CDC, NLC, and FIR) using the chain rule[6,7]. From learned γ_k, we can tell the nonlinear phase rotation which corresponds to the power of the signals at each point in the fibre[6]. Also, the inverse frequency responses of optical filters can be obtained by applying FFT to h_1 and h_2.

Experimental setup

The experimental setup and block diagram of offline Rx-DSP are shown in Fig. 1. A probabilistically-shaped 64-QAM 64-GBd signal is generated with the information rate of 3.305 bits and the entropy of 4.347 bits assuming a 21% FEC overhead[9]. The signal is Nyquist-shaped using a root-raised-cosine filter with a roll-off factor of 0.2. The frequency response (FR) of the transmitter is estimated in advance and compensated. A 120-GSa/s 4-ch arbitrary waveform generator (AWG) outputs the signal and 60-GHz driver amplifiers boosted it. A dual polarization IQ modulator (IQM) modulates continuous waves emitted from a micro-integrable tuneable laser assembly (µITLA) with a 40-kHz linewidth. The carrier wavelength is set to 192.7 THz. The optical signal is launched into a straight transmission line consisting of three spans of 50-km SSMF (α = 0.182 dB/km, D = 16.87 ps/nm/km). Each node has an optical bandpass filter (OBPF) and an erbium doped fibre amplifier (EDFA). The filters' centre frequency is varied from -20 GHz to 20 GHz with a 2-GHz granularity, and its bandwidth is set to 100 GHz. The fibre input power is set to 10 dBm at both two nodes.

At the receiver side, the signals are post-amplified by an EDFA and detected by a 90° hybrid and 100-GHz-bandwidth balanced photo detectors (BPDs). A 256-GSa/s digital sampling oscilloscope (DSO) with a 110GHz bandwidth digitizes the signal. In the Rx-DSP, the FR compensation and CDC are performed first, followed by polarization de-multiplexing with a one-tap adaptive equalizer with a butterfly configuration. After the frequency offset (FO) compensation[10] and carrier phase recovery (CPR)[11], the signal is divided into two paths for the learning of the coefficients h and γ_k,. One path is for the signal pre-processing, in which the compensated dispersion is re-applied. The other is for the reference signal generation for learning coefficients, which consists of the symbol decision and Nyquist filtering. Both the Tx and Rx DSP are performed in two samples

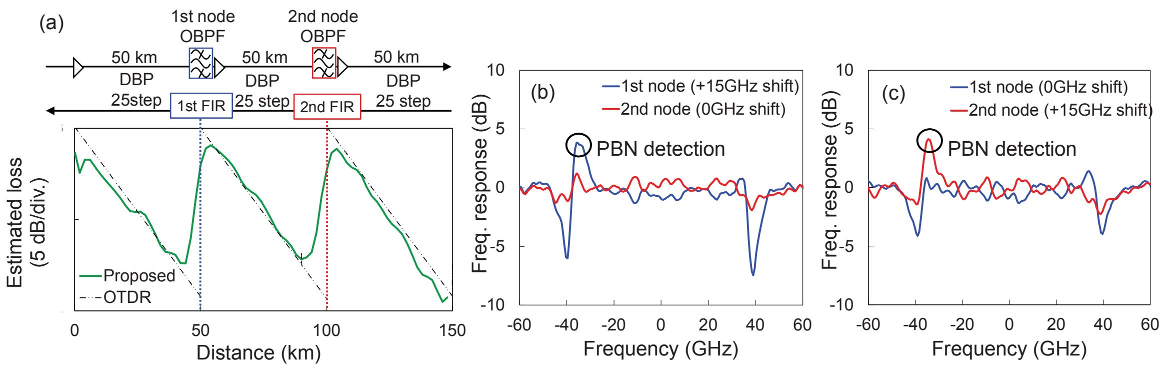

Fig. 2. (a) Loss profile estimated from learned γ_k in NLC block in DBP. Estimated frequency response from learned FIR filters h_1 and h_2 when only (a) the first and (b) second OBPF has the center frequency shifted by +15 GHz.

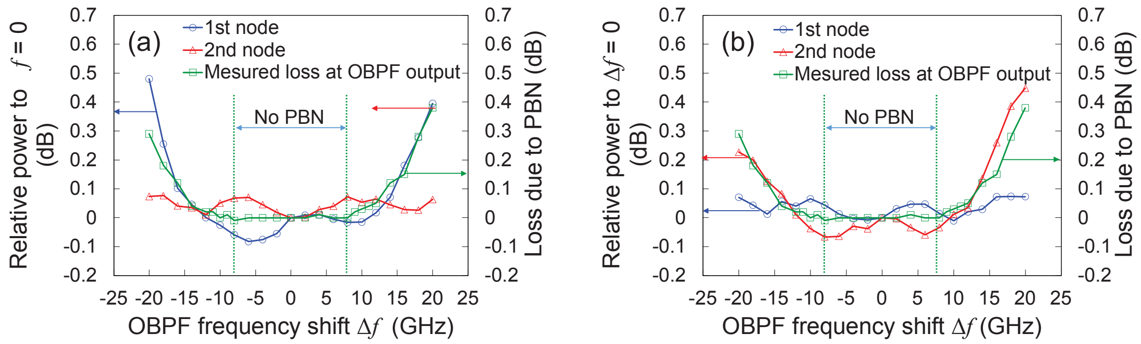

Fig. 3. Power of FIR filters $\Sigma|h(n)|^2$ (blue and red) and the measured loss at the OBPF output (green) when (a) the first and (b) second node of the OBPF are intentionally frequency-shifted by Δf and the other node has 0-GHz shift. The loss due to the PBN equals to the power of FIR filters because of a peak for PBN compensation (as can be seen in Fig. 2 (a) (b)).

per symbol. The pre-processed signal is fed into the proposed backpropagation and the length of each step (distance resolution) are set to 2 km.

Results and discussion

Figure 2 shows the estimated loss and frequency responses of complex FIR filters. The loss profile in Fig. 2 (a) is directly calculated from γ_k as $10\log_{10}\gamma_k$. The power profile measured by OTDR is also shown as a refrence. The fibre loss and amplification by EDFAs are successfuly observed. Fig. 2 (b) and (c) shows the FIR filter responses, when the center frequency of the OBPFs in the first and second nodes are shifted by +15 GHz, respectively. All the filters are shown in two samples per second. In Fig. 2 (b), the FIR filter h_1 (blue) has a peak that compensates for the PBN while the second one h_2 (red) exhibits a flat response, which clearly means the PBN occurs in the first node, not in the second node. The same tendency can be observed in Fig. 2 (c), where h_2 (red) has a peak, while h_1 does not. We can tell the PBN ocuurs only in the second node.

From the obtained FIR filters, the shifted frequency of OBPFs can also be estimated. A FIR with a peak has a larger power $\Sigma|h(n)|^2$ because of Parseval's identity $\Sigma|h(n)|^2 = \Sigma|H(m)|^2$, where $h(n)$ is the time domain expression of FIR and $H(m)$ is the frequency domain. Therefore, we can measure the loss due to the PBN by calculating the power of FIR filters. Fig. 3 shows the power of FIR filters $\Sigma|h(n)|^2$ (blue, red) and the loss due to the PBN measured right after the OBPF (green) as a function of the shifted frequency Δf. Note that the power and loss is relative value compared to when $\Delta f = 0$. Also, the moving average with a window of 3 is applied because the caculated tap power was noisy. Fig. 3 (a) and (b) corresponds to when only the first and second OBPF is shifted, respectively. In both cases, no loss was observed from -8 to 8 GHz shift since the filter bandwidth is approximately 100 GHz and no PBN occurs in that region. As the frequency shift increases, the measured loss becomes larger due to PBN. When only the first OBPF is shifted (Fig. 3 (a)), the power of h_1 has a good agreement to the measured loss because h_1 compensates for the PBN. On the other hand, the power of h_2 and the measured loss are less correlated, which implies the successful discrimination of the anomaly and normal OBPFs. In Fig. 3 (b), where only the second OBPF has the frequency shift, the power of h_2 has also the same tendency as the measured loss, while h_1 does not. When the Δf is -12 GHz < Δf < 10GHz, where less PBN occurs, two things are notable: (i) the powers of FIR filters are fluctuating. (ii) the two lines (blue and red) shows the reversed characteristics. (For example, when the power of h_1 is smaller than the measured loss, the power of h_2 shows the larger power.) The fluctuation is due to the bad convergence of the gradient method and this comes from other residual noises such as XY crosstalk (polarization demultiplexing has been perfromed using a one-tap adaptive equalizer), which is not fully compensated. The reason for (ii) is that, the total power of two FIR taps must be 1 (0 dB) when there is no PBN. If there is no PBN, the total response must show the unit impulse response.

Conclusion

We have proposed an optical-path backpropagation and its learning algorithm that can express the PBN in nodes using complex FIR filters. The method enables simultaneous estimation of the loss profile and PBN in multi-span link only using Rx-DSP. The estimated loss profile and PBN can be feed-backed to the network operator or directly to the actual device to fix the anomaly and will make the designing and managing system easier.

References

[1] P.J. Winzer et al., "Fiber-optic transmission and networking: the previous 20 and the next 20 years," Optics Express, 26(18), pp.24190-24239, 2018.

[2] P.S. Khodashenas et al., "Investigation of spectrum granularity for performance optimization of flexible Nyquist-WDM-based optical networks," *J. Lightw. Technol.*, *33*(23), pp.4767-4774, 2015.

[3] Y.T. Hsueh et al., "Passband narrowing and crosstalk impairments in ROADM-enabled 100G DWDM networks," J. Lightw. Technol. 30(24), pp. 3980-3986, 2012.

[4] D. Xie et al., "LCoS-Based Wavelength-Selective Switch for Future Finer-Grid Elastic Optical Networks Capable of All-Optical Wavelength Conversion," in IEEE Photonics Journal, 9(2), pp. 1-12, 2017.

[5] E. Ip, "Nonlinear Compensation Using Backpropagation for Polarization-Multiplexed Transmission," J. Lightw. Technol. 28(6), pp. 939-951, 2010.

[6] T. Sasai et al., "Simultaneous detection of anomaly points and fiber types in multi-span transmission links only by receiver-side digital signal processing." in Proc. of OFC2020, Th1F-1, 2020.

[7] C. Hager et al., "Nonlinear interference mitigation via deep neural networks," in Proc. of OFC 2018, W3A.4, 2018.

[8] D. P. Kingma and J. Ba, "Adam: A method for stochastic optimization," arXiv preprint arXiv:1412.6980, 2014.

[9] M. Nakamura et al., "Spectrally efficient 800 Gbps/carrier WDM transmission at 100-GHz spacing using probabilistically shaped PDM- 256QAM," in Proc. of ECOC 2018, We3G.5, 2018.

[10] Mengali, Umberto, and Michele Morelli. "Data-aided frequency estimation for burst digital transmission." IEEE transactions on communications, 45(1), pp.23-25, 1997

[11] T. Sasai et al., "Laser phase noise tolerance of uniform and probabilistically shaped QAM signals for high spectral efficiency systems." J. Lightw. Technol. 38(2), pp. 439-446, 2020.